EUKARYOTIC CELL, June 2002, p. 401–413 Vol. 1, No. 3
1535-9778/02/$04.00+0 DOI: 10.1128/EC.1.3.401–413.2002


# Differential Modulation of Cellular Signaling Pathways by Mild and Severe Hypovirus Strains

Todd B. Parsley, Baoshan Chen,† Lynn M. Geletka, and Donald L. Nuss*

*Center for Agricultural Biotechnology, University of Maryland Biotechnology Institute, College Park, Maryland 20742-4450*

Received 7 January 2002/Accepted 21 March 2002

**Hypoviruses persistently alter multiple phenotypic traits, stably modify gene expression, and attenuate virulence (hypovirulence) of their pathogenic fungal host, the chestnut blight fungus *Cryphonectria parasitica*. The pleiotropic nature of these changes is consistent with hypovirus-mediated perturbation of one or more cellular signal transduction pathways. We now report that two hypoviruses that differ in the severity of symptom expression differentially perturb specific cellular signaling pathways. The *C. parasitica 13-1* gene, originally identified as a hypovirus-inducible and cyclic AMP (cAMP)-regulated gene, was used to design a promoter-GFP reporter construct with which to monitor perturbation of cAMP-mediated signaling. Virus-mediated modulation of calcium/calmodulin/inositol trisphosphate-dependent signaling was monitored by measuring transcript accumulation from the *C. parasitica* laccase gene, *lac-1*. Infection by the severe hypovirus strain CHV1-EP713 caused a substantial induction of *13-1* promoter activity and a reduction of total extracellular laccase enzymatic activity (LAC-1 and LAC-3). In contrast, *13-1* promoter activity and total laccase activity were only marginally altered upon infection with the mild hypovirus strain CHV1-Euro7. However, examination of *lac-1*-specific transcript accumulation under previously defined culture conditions revealed that both CHV1-EP713 and CHV1-Euro7 perturbed calcium/calmodulin/inositol trisphosphate-dependent signaling. CHV1-EP713/CHV1-Euro7 chimeric viruses were used to map viral determinants responsible for modulation of cAMP-dependent signaling to domains within the central portion of the second open reading frame.**

Hypoviruses were initially discovered and have been extensively studied because they reduce the virulence (hypovirulence) of their fungal host, the chestnut blight fungus *Cryphonectria parasitica* (1, 35, 38, 39, 40, 51). However, it was observed early on in the characterization of hypovirulent *C. parasitica* field strains that phenotypic changes associated with hypovirus infection were not confined to virulence attenuation. Although different hypoviruses cause different constellations of phenotypic changes, the symptoms caused by a specific hypovirus are stable and generally consistent in different *C. parasitica* strain genetic backgrounds (1, 2, 4, 21, 22). For example, phenotypic changes associated with hypovirulence caused by the prototypic hypovirus CHV1-EP713 include reduced orange pigmentation, reduced asexual sporulation, and loss of female fertility (1, 2, 4, 21, 22).

The multiple phenotypic changes associated with hypovirus infection are accompanied by changes in the expression of specific cellular genes, e.g., the genes for laccase (16, 45), a sexual pheromone (54), the cell wall hydrophobin cryparin (56), a cellulobiohydrolase (53), a cutinase (52), and a polygalacturonase (23, 26). Using differential display, Chen et al. (12) provided evidence that hypovirus infection causes a rather extensive alteration in the host gene expression profile; more than 400 PCR products that either increased or decreased in abundance as a result of hypovirus infection were identified. The pleiotropic nature of these stable hypovirus-mediated changes in fungal phenotype and gene expression profiles suggested the possibility that hypovirus infection resulted in the perturbation of one or more key regulatory pathways.

The *C. parasitica lac-1* gene, encoding a laccase enzyme, has served as a useful reporter gene with which to examine the effects of hypovirus infection on fungal gene regulation. Several independent studies have shown that hypovirus infection causes a promoter-dependent reduction in *lac-1* transcript accumulation (16, 32, 45). Larson et al. (32) also provided evidence for two antagonistic pathways that govern *lac-1* transcription in virus-free *C. parasitica*. The first consists of a calcium/calmodulin/inositol trisphosphate-dependent stimulatory pathway. A second, negative regulatory pathway was shown to be sensitive to low levels of protein synthesis inhibitors and the immunosuppressant cyclosporin A (33). A comparison of the effects of a number of pharmacological agents and CHV1-EP713 infection on *lac-1* transcript accumulation led to the conclusion that virus-mediated suppression of *lac-1* transcription results from perturbation of the positive regulatory pathway (32).

Several independent lines of evidence have also suggested hypovirus-mediated perturbation of G-protein-regulated, cyclic AMP (cAMP)-mediated signal transduction. Choi et al. (15) reported the cloning of two *C. parasitica* Gα subunit genes, *cpg-1* and *cpg-2*, and that CHV1-EP713 infection resulted in a reduced accumulation of the *cpg-1* gene product, CPG-1. Chen et al. (12) subsequently reported elevated cAMP levels associated with hypovirus infection and the ability to mimic the effect of hypovirus infection on transcript accumulation for representative fungal genes by treatment with cAMP phosphodiesterase inhibitors. Targeted disruption of *cpg-1* was

* Corresponding author. Mailing address: Center for Agricultural Biotechnology, University of Maryland Biotechnology Institute, Plant Sciences Building, Room 5115, College Park, MD 20742-4450. Phone: (301) 405-0334. Fax: (301) 314-9075. E-mail: nuss@umbi.umd.edu.

† Present address: Biotechnology Research Center, Guangxi University, Nanning, Guangxi 530005, People's Republic of China.

reported by Gao and Nuss (24) to result in elevated cAMP levels and a set of phenotypic changes similar to but more severe than those caused by hypovirus infection.

These combined results established the requirement for an intact CPG-1 signaling pathway for optimal execution of a number of important fungal physiological processes, including virulence, and were consistent with the idea that a primary mechanism by which hypoviruses alter fungal virulence and phenotype involved perturbation of G-protein/cAMP signaling.

McCabe and coworkers (36, 37) have advanced the hypothesis that hypovirus infection impairs protein secretory pathways. This view is based on the observation that three fungal gene products downregulated by hypovirus infection, a sex pheromone (54), laccase (46), and cryparin (7), are each translated as preproteins that have recognition signals for processing during secretion by a Kex-2-like serine protease. This hypothesis suggests that by commandeering the vesicles of this secretory pathway for replication, hypoviruses impair protein secretion, leading to altered fungal phenotypes. As with most complex biological systems, it is likely that hypovirus infection perturbs multiple regulatory pathways and that interpretation is complicated by cross talk between pathways.

Efforts to identify hypovirus-encoded symptom determinants have been aided by the development of infectious cDNA clones of mild and severe hypovirus isolates CHV1-Euro7 and CHV1-EP713, respectively (14). By constructing chimeric viruses from the two infectious cDNA clones, Chen et al. (13) were able to fine-tune the interaction between *C. parasitica* and its plant host and map multiple viral determinants responsible for differences in colony and canker morphologies exhibited by fungal strains infected by the two hypoviruses. We now report that these two hypoviruses also differentially perturb cellular signaling pathways and demonstrate the use of promoter-reporter constructs to correlate hypovirus-mediated alteration in fungal phenotype with hypovirus-mediated alteration of specific cellular signaling cascades.

## MATERIALS AND METHODS

**Identification of *13-1* promoter sequence and construction of 13-1pGFP reporter plasmids.** Plasmid pPdEGFP, a *C. parasitica* promoter-reporter platform transformation vector, was created by replacing the 2,278–bp *Ssp*I-*Kpn*I fragment containing the *C. parasitica gpd* promoter and adjacent pUC19 sequence in pEGFP-CP (10, 50) with a promoterless 610-bp DNA fragment containing just the pUC19 vector sequence and unique restriction site recognition sequences for *Not*I and *Kpn*I restriction endonucleases. The 610-bp fragment was generated by polymerase chain amplification of pEGFP-CP DNA with oligonucleotides CPX-22mer (5′-CCTTTTTC**AATATT**ATTGAAGC-3′ [*Ssp*I restriction site in bold]) and CPX-42mer (5′-AAAA**GGTACC**AGGCCCT**GCGGCCGC**ACTGGCCGTC GTTTTAC-3′ [*Kpn*I and *Not*I restriction sites in bold]).

Following amplification, the 610-bp fragment was sequentially digested with *Ssp*I and *Kpn*I, gel purified, and incubated in the presence of T4 DNA ligase with the gel purified 6.8-kb *Ssp*I-*Kpn*I fragment of pEGFP-CP. The resulting plasmid, pPdEGFP, contained unique restriction sites for *Not*I and *Kpn*I abutted 5′ to the sequence encoding the *Aequorea victoria* enhanced green fluorescent protein (EGFP) (41) from Clontech plasmid pEGFP-1 (Clontech, Palo Alto, Calif.) that served as cloning sites for the insertion of fungal gene promoter elements. Both the pEGFP-CP and pPdEGFP transformation plasmids also contained the *Escherichia coli* hygromycin B phosphotransferase gene (*hph*) flanked by the *Aspergillus nidulans trpC* promoter and terminator.

The *13-1* promoter was isolated from a *C. parasitica* strain EP155 genomic library (λ-dash 15; Stratagene, La Jolla, Calif.). *E. coli* LE392 cells infected with the EP155 genomic library (16) were screened by in situ hybridization (47) with a randomly [α-$^{32}$P]dCTP-labeled *13-1* gene-specific DNA probe generated from the 800-bp *Eco*RV-*Bam*HI fragment of pUC19-13-1 (obtained from a differential mRNA display analysis [12]) by using the RTS RadPrime DNA Labeling System (Gibco-BRL, Rockville, Md.). Three positive plaques, λ1.4, λ2.1, and λ2.2, were identified and subjected to two rounds of plaque purification. λ phage DNA was isolated from the purified plaques, and the presence of the *13-1* sequence was verified by Southern blot analysis. *13-1* upstream sequences were then amplified from the λ1.4 and λ2.1 DNAs by PCR with either a T3- or T7-promoter specific primer (Novagen, Madison, Wis.), respectively, paired with OBC13-3 (5′-TCCCGTGAATAAGGAAGCG-3′), a *13-1*-specific primer that anneals to nucleotides 254 to 273 of the *13-1* coding region.

DNA fragments of ≈8.0 and 4.3 kb resulting from PCR amplification of λ1.4 and λ2.1 DNA, respectively, were gel isolated and subjected to automated DNA sequencing primed with the *13-1*-specific oligonucleotide 13-1R4 (5′-CTGATA ACAGCTTGGGAAA-3′ [anneals to nucleotides −160 to −141 relative to the 13-1 initiator AUG]) by using an ABI Prism automated DNA sequencer. Additional *13-1* upstream sequence was obtained from λ2.1 DNA by using a T7 promoter-specific primer. Based on the resulting DNA sequence, DNA oligonucleotides TP13-1NOTI (5′-ATAAG**GCGGCCGC**GAACTTAG-3′ [containing sequences encoded ≈3,200 nucleotides upstream of the *13-1* initiator AUG]) and TP13-1KPNI (5′-GTGTGCAG**GGTACC**CTAGGCTAG-3′ [complementary to nucleotides −68 to −45 relative to the *13-1* AUG initiator codon]) were synthesized (Gibco-BRL, Rockville, Md.) and used in PCR to amplify and engineer *Not*I and *Kpn*I restriction sites (in bold) into sequences upstream of the *13-1* coding region in λ2.1 DNA.

The resulting ≈3,200-bp PCR fragment was subjected to restriction endonuclease treatment with *Kpn*I and *Xmn*I to generate a 444-bp DNA fragment that was subsequently purified and incubated in the presence of T4 DNA ligase with the pPdEGFP vector that had been sequentially digested with *Not*I, treated with the Klenow fragment of DNA polymerase to fill in the recessed ends, and digested with *Kpn*I. The resulting plasmid, 13-1p(S)-GFP, contained 444 bp of *13-1* upstream sequence fused to the EGFP reporter coding sequence and was used to transform spheroplasts of *C. parasitica* strain EP155 (ATCC 38755 [18]). Positive transformants were selected for growth on potato dextrose agar (PDA [Difco Laboratories, Detroit, Mich.]) containing 40 μg of hygromycin B (Calbiochem, La Jolla, Calif.) per ml, and single conidia from positive transformants were isolated as previously described (19).

The integrity of the 13-1p(S)-GFP sequence was confirmed by PCR of total fungal DNA isolated from positive single conidia by using the method of Cenis (8) with oligonucleotides CPX-22mer and EGFP-1 (5′-TGTACAGCTCGTCC ATGC-3′ [complementary to nucleotides 697 to 714 of the EGFP coding sequence]). PCR-positive transformants were then screened for green fluorescence when grown on PDA supplemented with 2 mM theophylline or 2 mM caffeine (Sigma, St. Louis, Mo.). Single conidial isolate 13-1p(S)-GFP/EP155s.s.11, which was PCR and green fluorescence positive, was used for all subsequent analyses.

**In vitro transcription and transfection of 13-1p(S)-GFP/EP155s.s.11 with CHV1-EP713, CHV1-Euro7, and CHV1-EP713/Euro7 chimeric hypoviruses.** Spheroplasts were prepared from transgenic strain 13-1p(S)-GFP/EP155s.s.11 by the method of Churchill et al. (18) and diluted to a final concentration of $5 \times 10^6$ spheroplasts per ml in four parts STC, one part PTC, and dimethyl sulfoxide (DMSO) to 1% (final concentrations of 800 mM sorbitol, 100 mM Tris-HCl [pH 8.0], 100 mM $CaCl_2$, 8% polyethylene glycol 4000, and 1% DMSO), snap frozen in liquid nitrogen, and stored at −80°C.

Infectious synthetic transcripts of CHV1-EP713, CHV1-Euro7, and CHV1-EP713/Euro7 chimeric viruses R1, R2, R5, R10, R6, R12, R13, and R14 were generated from *Spe*I-linearized cDNA plasmid templates (13, 14) by using the Megascript transcription kit (Ambion, Austin, Tex.). The integrity of the resulting transcripts was verified by electrophoresis on a 0.8% agarose-TAE (Tris-acetate-EDTA) gel, and approximately 1 to 2 μg of each transcript was used to transfect $5 \times 10^5$ 13-1p(S)-GFP/EP155s.s.11 spheroplasts (11). Transfected spheroplasts were cultured on osmotic medium for 7 to 10 days to allow regeneration of cell walls and subsequently transferred to PDA for analysis. Virus-infected mycelial plugs from freshly transfected spheroplasts were then transferred to either PDA plates overlaid with cellophane or liquid medium (EP-complete [42] or potato dextrose broth [PDB; Difco Laboratories]) for molecular characterization.

**Visualization of GFP fluorescence.** Fluorescence analysis was performed on hyphae grown from fresh mycelial plugs inoculated adjacent to a sterile glass cover slip placed atop a PDA-cellophane plate with or without 2 mM caffeine or 2 mM theophylline. Following 3 days of growth at room temperature, cover slips along with freshly expanded mycelia were lifted from the cellophane and mounted inverted onto microscope slides prewetted with sterile distilled $H_2O$. Emission of green fluorescence was examined by using a Leica fluorescence stereomicroscope model MZ FLIII and a GFP plant fluorescent filter set (GFP3;

Leica Microscopy Systems, Heerbrugg, Switzerland). All fluorescent photographs were captured with a Spot 1.3.0 charge-coupled device digital camera (Diagnostic Instruments Inc., Sterling Heights, Mich.).

**Molecular analysis of GFP accumulation.** Immunoblot, Northern blot, and quantitative reverse transcription (RT)-PCR analyses were performed on total protein or RNA preparations extracted from freshly inoculated 50-ml EP-complete liquid medium cultures (plus or minus theophylline or caffeine for the final 48 h) or PDA plates (plus or minus theophylline or caffeine) overlaid with cellophane and grown for 6 to 7 days at 25°C. Mycelia from liquid cultures were collected on Miracloth (Calbiochem, La Jolla, Calif.) by using a Büchner funnel, blotted dry, and ground to a fine powder in liquid nitrogen in a chilled mortar. Mycelia cultured on PDA-cellophane plates was transferred directly to a chilled mortar with a spatula and ground to a fine powder in liquid nitrogen.

Protein was extracted from ground mycelia in TED buffer (100 mM Tris-HCl [pH 8.0], 1 mM EDTA, 0.5 mM EGTA, 10 mM dithiothreitol, 10 μg of aprotinin per ml, 10 μg of leupeptin per ml, and 2 mM phenylmethylsulfonyl fluoride) as previously described (25). Then 20 μg of total protein (determined by Bradford assay [6] by using the Bio-Rad protein assay kit [Bio-Rad, Hercules, Calif.]) from each sample was subjected to sodium dodecyl sulfate-polyacrylamide gel electrophoresis (SDS-PAGE) on a 12% polyacrylamide minigel (Bio-Rad, Hercules, Calif.) and transferred to an Immobilon-P membrane (Millipore, Bedford, Mass.) by using a Bio-Rad semidry transfer apparatus. The Immobilon-P membrane was then subjected to enhanced chemiluminescence (ECL) immunoblot analysis (Amersham Pharmacia, Piscataway, N.J.) according to the manufacturer's specifications with a 1:2,000 dilution of monoclonal anti-GFP antibody (Clontech, Palo Alto, Calif.) that had been cleared of nonspecific cross-reactivity to fungal lysate (25).

RNA was extracted from ground mycelia suspended in 4 ml of RNA extraction buffer (100 mM Tris-HCl [pH 8.0], 200 mM NaCl, 4 mM EDTA, 2 mM dithiothreitol, and 2% SDS). Nucleic acids were then subjected to sequential extractions with 4 ml of diethyl pyrocarbonate-$H_2O$-saturated phenol (pH 4.5), phenol-chloroform-isoamyl alcohol, and chloroform-isoamyl alcohol (47), and single-stranded RNA was precipitated on ice overnight with the addition of diethyl pyrocarbonate-treated LiCl to a final concentration of 2 M. Following LiCl precipitation, single-stranded RNA was treated with RQ-1 DNase (Promega, Madison, Wis.), phenol-chloroform extracted, and ethanol precipitated.

Northern blot analysis was performed on 10 μg of RNA from each sample following either treatment with glyoxal and resolution on a 1.2% agarose–10 mM sodium phosphate gel or denaturation with formaldehyde-formamide and resolution on a formaldehyde–morpholinepropanesulfonic acid (MOPS)–1% agarose gel, as indicated in the figure legends (47). Following verification of equal RNA loading and RNA integrity by staining with ethidium bromide, the RNA was transferred to a Nytran Plus membrane (Schleicher & Schuell, Keene, N.H.) by using capillary transfer in 10× SSC (1× SSC is 0.15 M NaCl plus 0.015 M sodium citrate) buffer. The RNA was cross-linked to the membrane by using a Stratalinker UV cross-linker (Stratagene, La Jolla, Calif.), and the membrane was subjected to hybridization overnight at 65°C with a gene-specific radiolabeled DNA probe generated by using High Prime labeling reagents (Boehringer, Mannheim, Germany) in hybridization buffer (1% SDS, 1 M NaCl, 10% dextran sulfate) or at 42°C in UltraHyb hybridization buffer (Ambion, Austin, Tex.).

Following hybridization, membranes were washed twice at room temperature with 2× SSC–0.1% SDS and twice with 0.2× SSC–0.1% SDS at 65°C or 42°C and exposed to X-ray film. Stripping of probe from membrane, when appropriate, was accomplished with two 15-min incubations in 100°C 0.1× SSPE (1× SSPE is 0.15 M NaCl, 10 mM $NaH_2PO_4$, and 1 mM EDTA)–0.1% SDS buffer, followed by a wash in 2× SSPE–0.1% SDS buffer at 25°C.

Quantitative RT-PCR was performed by using an Applied Biosystems (Foster City, Calif.) GeneAMP 5700 sequence detection system. A single cycle consisting of 5 min at 25°C, 30 min at 48°C, and 5 min at 95°C was used to reverse transcribe 50 to 100 ng of RQ-1 DNase-treated (Promega, Madison, Wis.) RNA in a reaction volume of 25 to 50 μl by using Applied Biosystems TaqMan reverse transcription reagents (final concentrations: 10 mM Tris-HCl [pH 8.3], 50 mM KCl, 5.5 mM $MgCl_2$, 500 μM each deoxynucleoside triphosphate [dNTP], 2.5 μM random hexamer, 0.4 U of RNase inhibitor, and 1.25 U of Multiscribe reverse transcriptase per ml).

Five microliters of cDNA was then subjected to quantitative real-time PCR with TaqMan master-mix reagents (Applied Biosystems, Foster City, Calif.) in a total reaction volume of 25 μl with either a *gfp*-specific TaqMan probe and primer set (probe: 5′-6FAM-AAAGACCCCAACGAGAAGCGCGA-TAMRA-3′ [6FAM, 6-carboxyfluorescein; TAMRA, 6-carboxytetramethylrhodamine] [nucleotides 627 to 649 of the EGFP coding sequence]; forward primer: 5′-CTGCTGCCCGACAACCA-3′ [nucleotides 582 to 598 of the EGFP coding sequence]; reverse primer: 5′-GAACTCCAGCAGGACCATGTG-3′ [complementary to nucleotides 651 to 671 of the EGFP coding sequence]) or a *13-1* gene-specific TaqMan probe and primer set (probe: 5′-6FAM-CGAGGCG-CACGCTTCCTTATTCAC-TAMRA-3′ [nucleotides 166 to 188 of the *13-1* coding sequence]; forward primer: 5′-GCATCAATGTGACCGTGGTTT-3′ [nucleotides 138 to 157 of the *13-1* coding sequence]; reverse primer: 5′-GCCTTCTC CTCCCGCTTTT-3′ [complementary to nucleotides 192 to 210 of the *13-1* coding sequence]) designed by using Primer Express software (Applied Biosystems, Foster City, Calif.). Optimal final concentrations for TaqMan primer and probe sets were determined empirically as 100 nM for the TaqMan probe and 200 nM for each of the forward and reverse primers.

The abundance of *gfp* or *13-1* transcript in each sample was normalized by using the comparative ΔCt method (28) relative to the amount of 18S rRNA in the sample, determined as above by using 2 μl of a 1:1,000 dilution of cDNA and 18S rRNA gene-specific probe and primers (probe: 5′-6FAM-TTCTGGGCCG CACGCGC-TAMRA-3′; forward primer: 5′-ATAACAGGTCTGTGATGCCC TTAGA-3′; reverse primer: 5′-CTCGCTGGCTCTGTCAGTGTAG-3′). The 18S rRNA forward primer sequence was designed to span the insertion site of a 547-bp intron found within the *C. parasitica* 18S gene (9) so that only fully processed 18S cDNA was amplified in the quantitative RT-PCR.

**Analysis of *lac-1* transcript accumulation in 13-1(S)-GFP/EP155 infected with CHV1-EP713/Euro7 chimeric viruses.** Qualitative analysis of extracellular laccase (*Lac*1 and *Lac*3 [43, 46]) activity was performed on fresh mycelial plugs transferred from 5-day-old PDA cultures to Bavendamm's medium (5) and grown in the dark at 25°C for 6 days. The effect of hypovirus infection on the specific accumulation of *C. parasitica lac-1* transcript was monitored by Northern blot analysis (32) and quantitative RT-PCR by using *lac-1*-specific primers (16) (forward primer: 5′-CACTCTCACTTCTCGGCACAATAC-3′ [nucleotides 510 to 534 of the LAC-1 cDNA sequence]; reverse primer: 5′-ACTGGCAGGACC GTCAATCT-3′ [complementary to nucleotides 561 to 580 of the LAC-1 cDNA sequence]), and probe (5′-6FAM-CGGCATCGTCGGCGCCAT-TAMRA-3′ [nucleotides 540 to 559 of the LAC-1 cDNA sequence]; Integrated DNA Technologies, Coralville, Iowa) as described above for the *13-1* gene product. For these analyses, total RNA was extracted from mycelia recovered from 50-ml potato dextrose broth (PDB) liquid cultures pulsed with either 1.5% malt extract for 12 h or 3 μM cycloheximide for up to 24 h as described by Larson et al. (32).

## RESULTS

**Isolation and characterization of the *13-1* promoter.** The *13-1* gene was originally identified by differential mRNA display analysis as encoding a transcript that was inducible either after hypovirus infection or following treatment with cAMP phosphodiesterase inhibitors. Consequently, the *13-1* promoter provided a potential tool for monitoring hypovirus-mediated modulation of cAMP-regulated gene expression. Three independent recombinant λ phages containing the *13-1* sequence were initially identified by probing a λ-dash EP155 genomic library with the *13-1*-specific probe recovered from the differential display analysis (12).

Informational and molecular analysis of the *13-1* gene revealed the following details: the predicted coding domain consisted of 122 codons with no prospective introns, and two putative TATA box elements were found at positions −138 to −130 and −111 to −105, relative to the initiator AUG. Targeted disruption of the *13-1* gene resulted in no detectable phenotypic changes (data not shown). No significant matches were observed when the predicted 13-1 amino acid sequence was compared with existing protein sequence databases.

A 444-bp portion of the *13-1* gene promoter extending from positions −35 to −339 relative to the *13-1* initiator AUG codon was fused to the coding region of the *Aequorea victoria* enhanced green fluorescence protein (EGFP) gene (41) in plasmid pPdEGFP. This plasmid was then used to produce a transgenic *C. parasitica* promoter-GFP reporter strain, 13-1p(S)-GFP/EP155, which contained chromosomally integrated

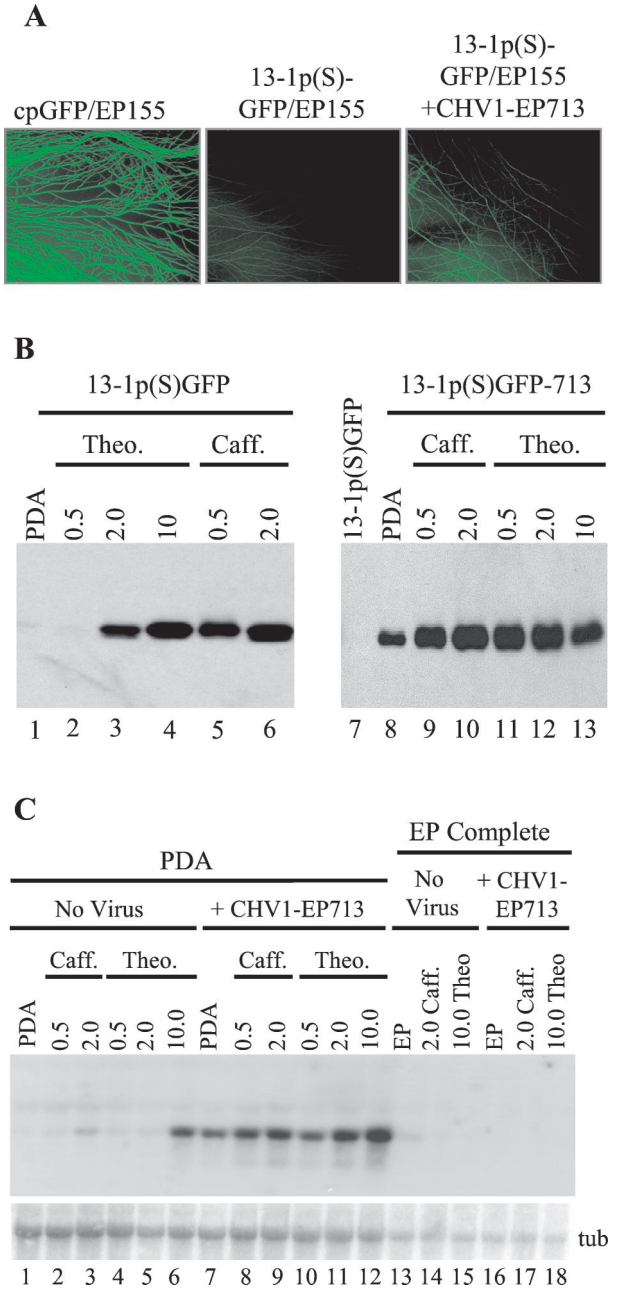


FIG. 1. Accumulation of EGFP in the *C. parasitica* transgenic reporter strain 13-1p(S)-GFP/EP155 in response to infection with CHV1-EP713 and/or the presence of the phosphodiesterase inhibitor caffeine (Caff.) or theophylline (Theo.). (A) Green fluorescence analysis of uninfected (center) and CHV1-EP713-infected (right) 13-1p(S)-GFP/EP155 compared with cpGFP/EP155, a transgenic *C. parasitica* strain containing a copy of the EGFP coding sequences under the transcriptional control of the constitutive *C. parasitica gpd* promoter (left) (50). All exposure times were standardized to that of the positive control by using the imaging software provided with the Spot 1.3.0 charge-coupled digital device camera. (B) Immunoblot analysis with anti-GFP of uninfected (lanes 1 to 7) or CHV1-EP713-infected (lanes 8 to 13) 13-1p(S)-GFP/EP155 cultured on PDA-cellophane in the absence (lanes 1, 7, and 8) or presence of increasing concentrations of theophylline (lanes 2 to 4 and 11 to 13) or caffeine (lanes 5, 6, 9, and 10). (C) Northern blot analysis of uninfected (lanes 1 to 6 and 13 to 15) or CHV1-EP713-infected (lanes 7 to 12 and 16 to 18) 13-1p(S)-GFP/EP155 cultured on PDA-cellophane (lanes 1 to 12) or EP-complete liquid medium (lanes 13 to 18) in the absence (lanes 1, 7, 13, and 16) or presence of increasing concentrations of caffeine (lanes 2, 3, 8, 9, 14, and 17) or theophylline (lanes 4 to 6, 10 to 12, 15, and 18). For the bottom panel, the membrane was stripped and reprobed for β-tubulin (tub). Concentrations (millimolar) of caffeine and theophylline are indicated above each lane in both panels B and C.

copies of the EGFP coding region under the presumptive transcriptional control of a functional *13-1* promoter.

As indicated in Fig. 1A, an increase in green florescence was observed in the transgenic reporter strain in response to CHV1-EP713 infection or cAMP phosphodiesterase inhibitors (data not shown). Fluorescent microscopic analysis was augmented with molecular analysis throughout this study to verify the effect of hypovirus infection or cAMP phosphodiesterase inhibitors on the accumulation of reporter GFP protein and/or transcript. Treatment with either theophylline or caffeine or infection by the prototypic CHV1-EP713 strain of hypovirus resulted in increased accumulation of the GFP reporter protein and mRNA (Fig. 1). GFP accumulation in response to the phosphodiesterase inhibitors was dose dependent (lanes 2 to 6, Fig. 1B and 1C), suggesting that elevated 13-1pGFP expression was a result of increased intracellular cAMP (12).

The combination of CHV1-EP713 infection and phosphodiesterase inhibitors resulted in an additive increase in GFP protein and transcript accumulation that was greater than that observed in response to CHV1-EP713 infection or phosphodiesterase inhibitors alone (Fig. 1B, lanes 9 to 13; Fig. 1C, lanes 8 to 12). Stimulation of 13-1pGFP was also dependent on growth conditions. Neither GFP protein (data not shown) or mRNA nor endogenous *13-1* message (data not shown) was detected when the reporter strain was cultured in liquid medium in the presence of CHV1-EP713 and/or phosphodiesterase inhibitors (Fig. 1C, lanes 13 to 18). The influence of culture conditions on *13-1* promoter-dependent transcript accumulation will be addressed in detail in a subsequent section.

The RNA expression profile of the reporter 13-1p(S)-GFP transcript mimicked that of the endogenous *13-1* mRNA in response to phosphodiesterase inhibitors and infection with CHV1-EP713 (12) (data not shown). These results validate the utility of the 13-1p(S)-GFP/EP155 reporter strain for monitoring the impact of hypovirus infection on cAMP-mediated promoter-dependent induction of cellular gene expression.

**Severe and mild hypovirus strains differentially modulate a cAMP-regulated gene expression pathway.** Hypovirus CHV1-Euro7 shows extensive sequence identity with CHV1-EP713 at both the amino acid level (90 to 98% identity) and at the nucleotide level in the 5′ and 3′ noncoding sequences (93% identity). However, CHV1-Euro7 and CHV1-EP713 confer distinct phenotypes on infected *C. parasitica* strains. CHV1-EP713 can be classified as a severe hypovirus strain, causing a greater reduction in fungal growth rate on synthetic medium and more severely attenuating both the development of spore-containing stromal pustuales (asexual sporulation) and canker expansion on chestnut tissue than the milder CHV1-Euro7 strain (14). The high degree of sequence identity coupled with the differences in symptom severity between the two hypovirus strains stimulated the construction of infectious CHV1-EP713/Euro7 chimeric viruses and the use of these chimeras to map specific regions of the viral genome as symptom determinants

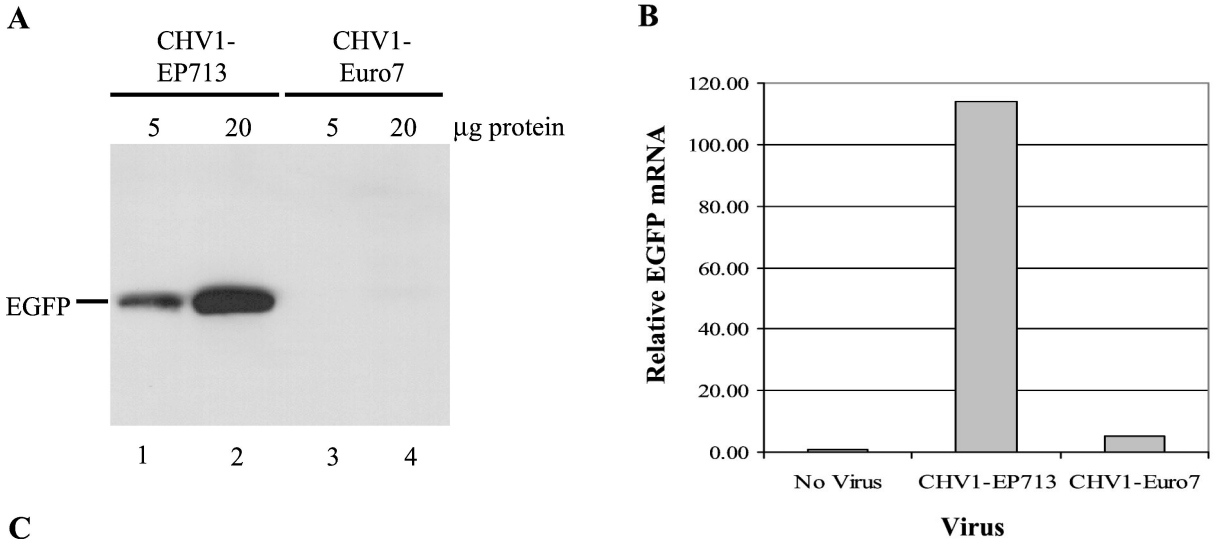


FIG. 2. GFP accumulation in 13-1p(S)-GFP/EP155 infected with CHV1-EP713 or CHV1-Euro7. (A) Immunoblot analysis with anti-GFP of 5 or 10 µg of total protein from 13-1p(S)-GFP/EP155 infected with either CHV1-EP713 (lanes 1 and 2) or CHV1-Euro7 (lanes 3 and 4). (B) Real-time semiquantitative RT-PCR analysis of EGFP mRNA accumulation in uninfected and CHV1-EP713- or CHV1-Euro7-infected 13-1p(S)-GFP/EP155. All values for EGFP mRNA in panel B were normalized to total 18S rRNA in each sample as described in Materials and Methods and are expressed as fold accumulation relative to the amount of EGFP mRNA present in virus-free 13-1p(S)-GFP/EP155. (C) Immunoblot analysis of GFP accumulation in virus-free (lanes 1 to 3), CHV1-Euro7-infected (lanes 4 to 6), or CHV1-EP713-infected (lanes 7 to 9) 13-1p(S)-GFP/EP155 cultured on PDA-cellophane in the absence (0) (lanes 1, 4, and 7) or presence of 2 mM caffeine (C, lanes 2, 5, and 8) or 2 mM theophylline (T, lanes 3, 6, and 9).

conferring changes in canker morphology, growth rate, and sporulation (13, 14, 20).

As shown in Fig. 2, while CHV1-EP713 infection of 13-1p(S)-GFP/EP155 resulted in elevated accumulation of GFP, infection with CHV1-Euro7 did not. This difference was expressed quantitatively by using real-time RT-PCR (Fig. 2B) and indicated that accumulation of *gfp* message in the CHV1-EP713-infected strain was 15- to 20-fold higher than in the CHV1-Euro7-infected strain (and in excess of 90-fold higher than in the virus-free strain). Importantly, although CHV1-Euro7 infection alone did not lead to detectable GFP accumulation, the CHV1-Euro7-infected strain was not refractory to GFP accumulation when cultured in the presence of caffeine or theophylline (Fig. 2C, lanes 4 to 6). This suggests that CHV1-Euro7 does not repress cAMP-mediated activation of the 13-1 pathway, but rather that the pathway is stimulated by CHV1-EP713 and increased levels of intracellular cAMP (12).

The marked difference in activation of the 13-1 pathway exhibited by the phenotypically severe (CHV1-EP713) and mild (CHV1-Euro7) hypovirus strains provided a platform for the mapping of CHV1-EP713 viral determinants modulating cAMP-dependent cellular gene regulation through the use of infectious CHV1-EP713/CHV1-Euro7 chimeras (13, 14).

**Virus-mediated activation of the 13-1 pathway maps to the region of CHV1-EP713 encoding the putative RNA-dependent RNA polymerase.** The genome of hypovirus species CHV1 contains two contiguous open reading frames, ORF A and ORF B (14, 48) (Fig. 3A). ORF A encodes a polyprotein of 69 kDa that is autocatalytically processed by a papain-like proteinase encoded within its N terminus into the mature viral proteins p29 and p40 (17, 49). The second open reading frame, ORF B, encodes a polyprotein of greater than 300 kDa in mass (48). Like ORF A, ORF B is autocatalytically processed by a papain-like proteinase activity encoded in its N terminus. This processing event results in the release of the N-terminal p48 proteinase (49). Other proteolytic processing events occurring within ORF B and the resulting mature viral products have yet to be identified; however, based on sequence similarities and alignments with conserved domains of single-stranded RNA viruses, domains encoding a putative RNA-dependent RNA polymerase and an RNA helicase have been identified (31).

Previous phenotypic characterization of chimeric viruses A713BE7 and AE7B713 (R1 and R2, respectively, in this study [Fig. 3A]) indicated that the primary determinants responsible for the differences in symptom expression observed between CHV1-EP713 and CHV1-Euro7 were located within ORF B (14). Further dissection of ORF B symptom expression deter-

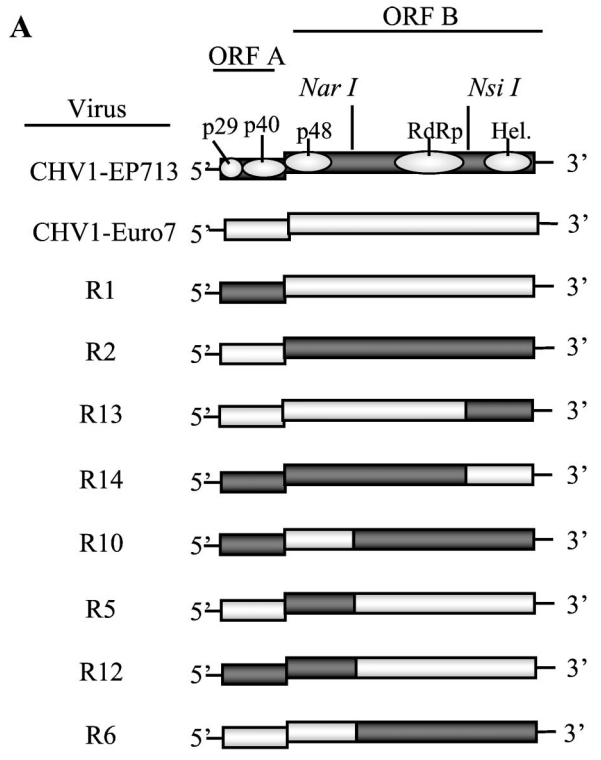


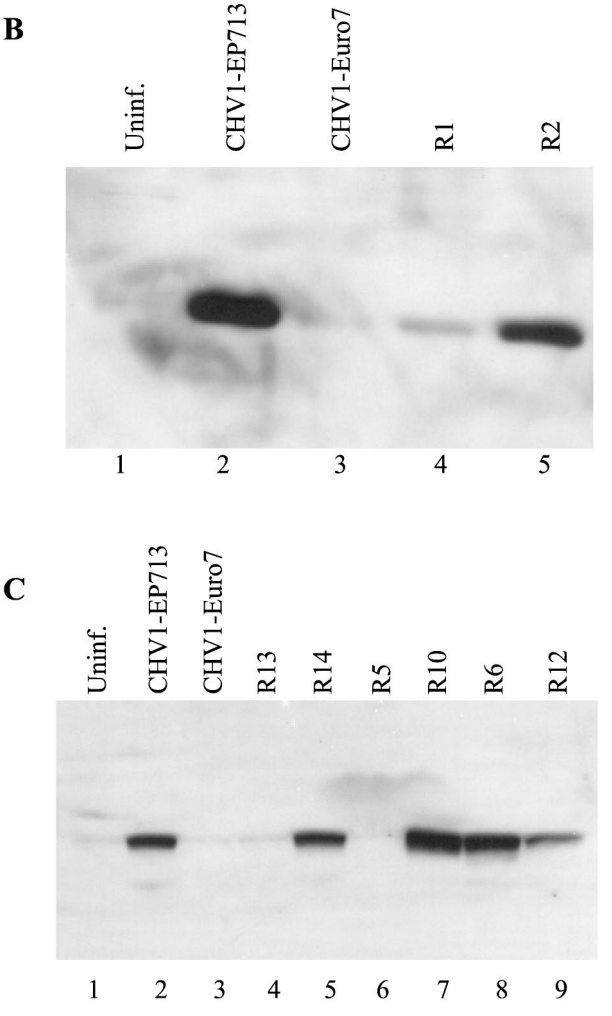


FIG. 3. Accumulation of GFP in 13-1p(S)-GFP/EP155 infected with CHV1-EP713 and CHV1-Euro7 chimeric viruses. (A) Diagrammatic representation of chimera genomes. Shaded boxes represent portions of the chimera containing CHV1-EP713 sequence. Open boxes represent CHV1-Euro7 sequence. *Nar*I and *Nsi*I restriction sites at nucleotides 5310 and 9897, respectively, used in the engineering of chimeras and virus-encoded protein domains are indicated at the top of the figure (adapted from Chen et al. [13]). (B) Immunoblot analysis with monoclonal anti-GFP of 20 μg of total protein extracted from 13-1p(S)-GFP/EP155 infected with CHV1-EP713 (lane 2), CHV1-Euro7 (lane 3), R1 (lane 4), or R2 (lane 5). Lane 1, 20 μg of total protein from virus-free 13-1p(S)-GFP/EP155. (C) Immunoblot analysis with monoclonal anti-GFP of 20 μg of total protein extracted from 13-1p(S)-GFP/EP155 infected with CHV1-EP713 (lane 2), CHV1-Euro7 (lane 3), R13 (lane 4), R14 (lane 5), R5 (lane 6), R10 (lane 7), R6 (lane 8), or R12 (lane 9). Lane 1, 20 μg of total protein from virus-free 13-1p(S)-GFP/EP155.

minants resulted in the identification of CHV1-EP713-encoded domains specifying characteristic traits in canker morphology, growth rate, and suppression of asexual sporulation (13). To begin linking identified hypovirus symptom determinants to modulation of specific host signaling pathways, we examined the accumulation of GFP in 13-1p(S)-GFP/EP155 infected with a panel of reciprocal CHV1-EP713/Euro7 chimeras (Fig. 3A).

As shown in Fig. 3B, infection of strain 13-1p(S)-GFP/EP155 with the R2 chimera resulted in the accumulation of GFP protein to levels approaching that observed for the CHV1-EP713 infection (Fig. 3B, lanes 2 and 5). Similarly, infection with chimera R1 resulted in the minimal GFP accumulation observed following CHV1-Euro7 infection (Fig. 3B, lanes 3 and 4). Thus, the primary viral determinants mediating induction of the 13-1 pathway also reside within CHV1-EP713 ORF B. Chimeric viruses constructed at the *Nsi* I site (R13 and R14, Fig. 3A) also induced GFP protein accumulation similar to the parental viruses from which the region upstream of the *Nsi* I site was derived. That is, R13 induced GFP protein accumulation similar to CHV1-Euro7, while R14 performed similar to CHV1-EP713 (Fig. 3C), narrowing the region of ORF B responsible for the differences in induction of the 13-1 pathway to between the N terminus (nucleotide 2363) and nucleotide 9897. Moreover, the correlation between induction of *13-1* promoter activity and symptom severity, e.g., altered colony morphology and suppression of asexual sporulation on cankered chestnut tissue, observed for the parental viruses was maintained with this set of reciprocal chimeric viruses. Chimeric viruses previously shown by Chen et al. (13) to produce CHV1-EP713-like symptoms, R2 and R14, induced GFP accumulation, while the chimeras that produced CHV1-Euro7-like symptoms, R1 and R13, did not.

The region between nucleotides 2363 and 9897 was further dissected by using reciprocal chimeras R5-R10 and R6-R12, constructed at the *Nar* I restriction site (Fig. 3A). Significant GFP protein accumulation was observed in mycelia infected with the two chimeras (R6 and R10) that contained CHV1-EP713 sequences downstream of the *Nar*I site, but not in mycelia infected with chimeras R5 and R12, which contained

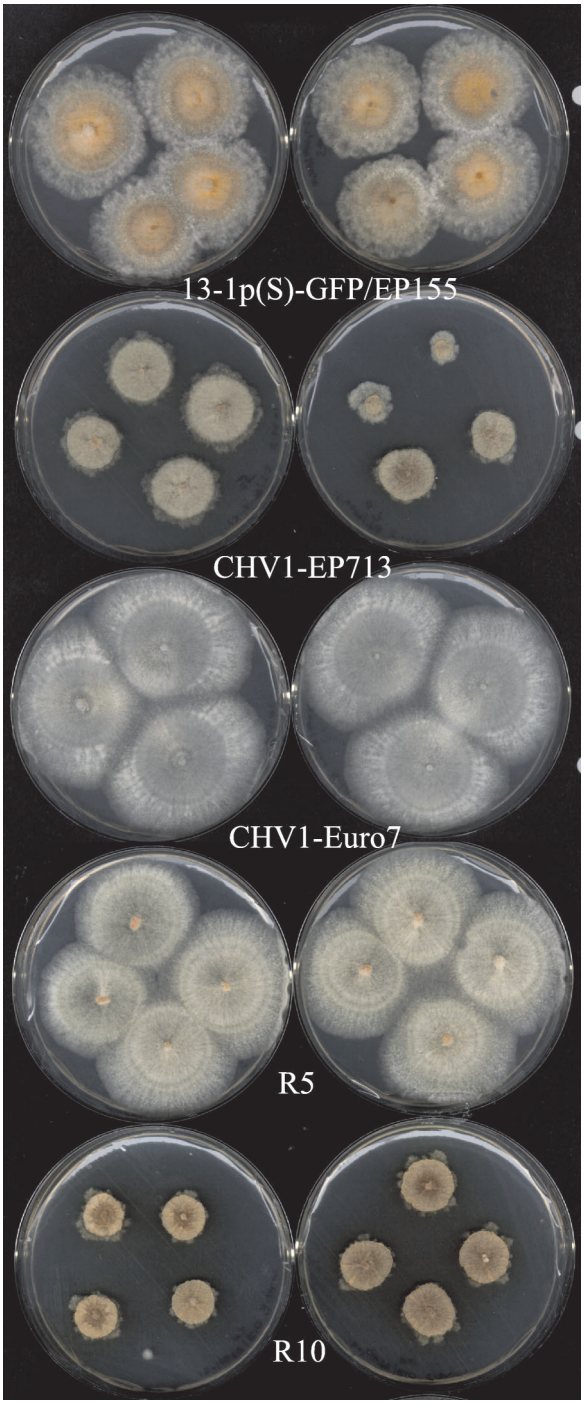


FIG. 4. Phenotypes of 6-day-old PDA-cellophane cultures of virus-free (top) and virus-infected 13-1p(S)-GFP/EP155 (as indicated) mycelia, in duplicate. Plates were scanned on a Hewlett-Packard flat scanner just prior to harvesting of protein for immunoblot analysis.

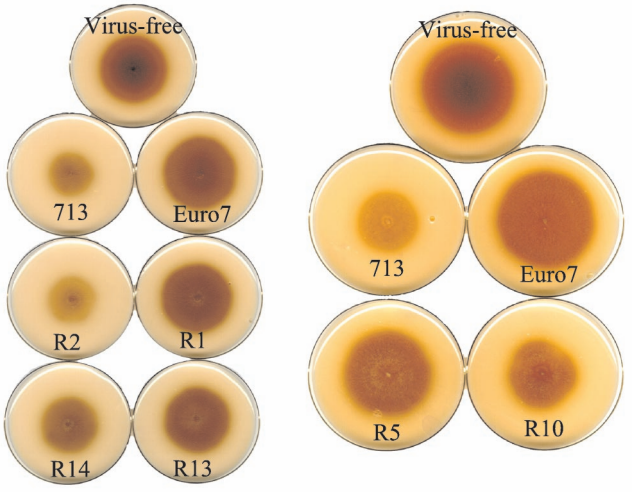


FIG. 5. Laccase activity of virus-free and hypovirus-infected 13-1p(S)-GFP/EP155 on Bavendamm's medium. Plates were scanned as described for Fig. 4.

CHV1-EP713 sequences upstream of the *Nar*I site (nucleotides 2363 to 5310) (Fig. 3C). Thus, to a first approximation, primary determinants responsible for CHV1-EP713-mediated induction of the 13-1 pathway reside between ORF B nucleotides 5310 and 9897, a region that includes the virus-encoded RNA-dependent RNA polymerase. However, the observation that some minor accumulation of the GFP reporter was observed in R12-infected but not in R5-infected mycelia also raises the possibility that CHV1-EP713 nucleotides 2363 to 5310 could, in conjunction with the homologous ORF A sequences, contribute to a low level of *13-1* induction.

Chen et al. (13) reported that chimeric viruses R5, R10, R6, and R12 all caused CHV1-EP713-like colony morphologies on PDA medium when transfected into *C. parasitica* strain EP155. However, when cultured on PDA-cellophane, conditions used in this study to allow harvesting of mycelia for extraction of protein and nucleic acids, strain 13-1p(S)-GFP/EP155 infected with the reciprocal chimeric viruses exhibited quite distinct colony morphologies (Fig. 4). R5- and R12-infected 13-1p(S)-GFP/EP155 formed colonies similar to CHV1-Euro7-infected mycelia, while R6- and R10-infected colonies resembled the severe CHV1-EP713-like morphology (Fig. 4 and data not shown).

Thus, the CHV1-EP713 region between nucleotides 5310 and 9897 contains determinants for both reduced radial growth on PDA-cellophane and induction of the cAMP-mediated *13-1* pathway. However, the correlation between *13-1* induction in PDA-cellophane-grown mycelia and the previously described virus-mediated suppression of pustule formation on chestnut cankers observed for the parental viruses and reciprocal chimeras R1-R2, and R13-R14 did not extend to the R5-R10 and R6-R12 reciprocal chimeras. Direct measurement of *13-1* promoter-dependent GFP accumulation in cankered chestnut tissue was not technically feasible.

**Severe and mild hypoviruses differentially reduce overall laccase enzymatic activity but display similar abilities in disrupting calcium/calmodulin/inositol trisphosphate-dependent signaling under defined growth conditions.** Suppression of laccase enzymatic activity has long been a hallmark of hypovirus-mediated disruption of fungal gene expression (1, 32, 45, 46). The relative level of extracellular laccase activity produced by virus-free and hypovirus-infected *C. parasitica* strains can be qualitatively examined by culturing the strains on Bavendamm's medium (1.5% [wt/vol] malt extract, 0.5% [wt/vol]

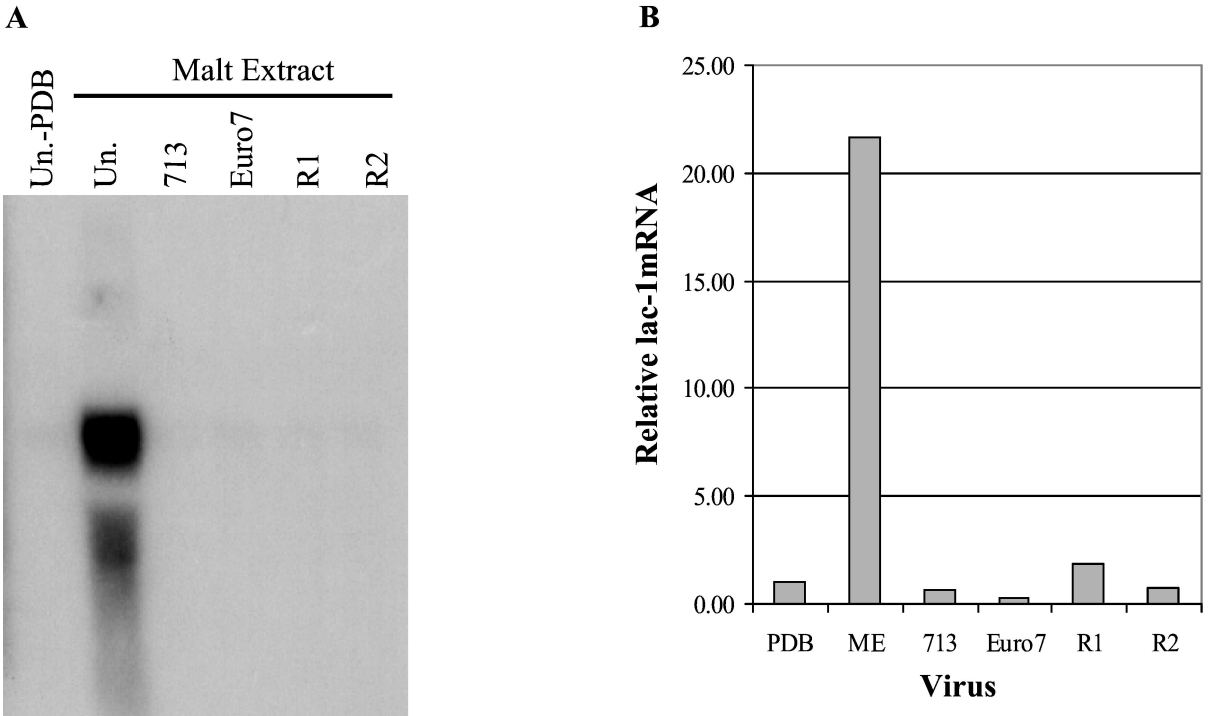


FIG. 6. Accumulation of *lac-1* transcript in 13-1p(S)-GFP/EP155 grown in 1.5% (wt/vol) malt extract. Uninfected and virus-infected (as indicated at the top of the figure) mycelia were initially cultured in PDB, and then medium was switched to either fresh PDB (lane 1) or 1.5% (wt/vol) malt extract (lanes 2 to 6). Mycelia were harvested for RNA extraction following 12 h of incubation in the dark at room temperature. (A) A total of 10 μg of total RNA was denatured and resolved on a 1% agarose–formaldehyde gel. The RNA was then transferred to a positively charged Nytran membrane and hybridized with a radiolabeled *lac-1*-specific probe. (B) *lac-1* mRNA accumulation was also quantified by real-time RT-PCR by using specific TaqMan probe and primers as described in Materials and Methods. The *y* axis indicates relative *lac-1* accumulation normalized to 18S rRNA.

tannic acid, and 2% agar [44]). Virus-free *C. parasitica* strains produce a dark brown color as a result of the breakdown of phenolic compounds by the phenolic oxidase activity of extracellular laccase enzymes LAC-1 and LAC-3 (43).

As shown in Fig. 5, infection of 13-1p(S)-GFP/EP155 with CHV1-EP713 resulted in nearly complete suppression of extracellular laccase activity, while the CHV1-Euro7-infected strain was still able to produce active laccase to nearly virus-free levels. The differential suppressive activity displayed by the R1 and R2 chimeras suggested that the viral determinant of laccase suppression maps to CHV1-EP713 ORF B. Further dissection of potential ORF B determinants mediating suppression of laccase activity was inconclusive, as evidenced by the nearly equal intensity of brown coloration between the R13 and R14 and the R5 and R10 chimera-infected 13-1p(S)-GFP/EP155 cultures.

The severe hypovirus strain CHV1-EP713 was previously reported to suppress a calcium/calmodulin/inositol trisphosphate pathway that positively regulates the accumulation of *lac-1* transcripts (32). Culture conditions defined by Larson et al. (32) for monitoring both positive and negative regulation of *lac-1* transcript accumulation provided an opportunity to test whether the differential suppression of extracellular laccase activity by CHV1-EP713 and CHV1-Euro7 observed on Bavendamm plates correlated with a differential suppression of the calcium/calmodulin/inositol trisphosphate-dependent signal transduction pathway.

As shown in Fig. 6A and 6B, a switch in growth medium from nutrient-rich potato dextrose broth to liquid medium composed solely of 1.5% (wt/vol) malt extract induced a robust accumulation of *lac-1* transcript in virus-free 13-1p(S)-GFP/EP155. This calcium/calmodulin/inositol trisphosphate-mediated induction of *lac-1* transcript accumulation was repressed by both the severe and mild strains of hypovirus. The combination of heterologous ORF A and ORF B coding sequences represented by the R1 and R2 chimeras did not alter the ability of the viruses to repress *lac-1* accumulation through this pathway. As shown in Fig. 9, both CHV1-EP713 and CHV1-Euro7 were also able to suppress *lac-1* transcript accumulation caused by derepression of the negative-acting pathway through the addition of cycloheximide. Thus, no evidence for differential perturbation of calcium/calmodulin/inositol trisphosphate signaling by the mild and severe hypovirus strains was observed under defined culture conditions developed to specifically monitor hypovirus-mediated suppression of *lac-1* transcript accumulation.

**Separate pathways regulate *13-1* and *lac-1* expression.** Additional insights into the regulation of *13-1* and *lac-1* expression were obtained by direct comparison of the relative accumulation of endogenous *13-1* and *lac-1* transcripts under a variety of growth conditions. As shown in Fig. 7, *13-1* tran-

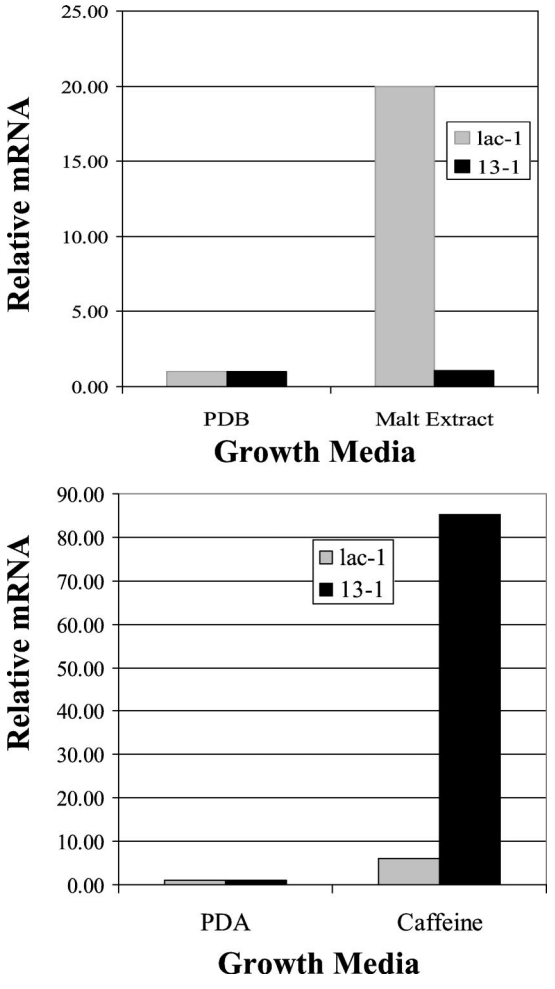


FIG. 7. Real-time semiquantitative RT-PCR analysis of *lac-1* and *13-1* transcripts under different growth conditions. Total RNA isolated from virus-free 13-1p(S)-GFP/EP155 cultured in PDB or 1.5% (wt/vol) malt extract for 12 h (upper panel) after an initial incubation in PDB or on PDA plates minus or plus 2 mM caffeine for 6 days (lower panel) was subjected to real-time RT-PCR with *lac-1*-specific TaqMan probe and primers (light shaded bars) or *13-1*-specific TaqMan probe and primers (dark shaded bars).

scripts failed to accumulate under the culture conditions developed to monitor calcium/calmodulin/inositol trisphosphate-mediated induction of *lac-1* expression; a switch from rich liquid medium to 1.5% malt extract. Similarly, the large induction in *13-1* expression observed for PDA-cellophane-grown mycelia treated with the phosphodiesterase inhibitor caffeine was not accompanied by an increase in *lac-1* transcript accumulation. The observation that two cellular genes that are independently regulated in uninfected cells are either induced (*13-1*) or suppressed (*lac-1*) as a result of hypovirus infection supports the view that hypovirus infection alters multiple independent regulatory pathways.

Data presented in Fig. 1C (lanes 13 to 18) indicated that activation of the *13-1* pathway was also influenced by culture conditions. The greater than 80-fold increase in *gfp* or endogenous *13-1* transcript accumulation observed for CHV1-EP713-infected and caffeine-treated mycelia grown on PDA-cellophane was not observed in liquid medium (EP-complete, Fig. 1C, lanes 16 and 17; PDB, Fig. 8A, lane 1, lower panel; minimal medium, data not shown). These results suggest the possibility of some form of liquid medium-dependent repression of *13-1* induction. Further analysis showed that repression of *13-1* expression could be relieved by the addition of cycloheximide independent of virus infection (Fig. 8A and 8B, bottom panels, and Fig. 9, bottom panel, lanes 1 to 3). This result suggests a need for on-going protein synthesis of a transient transcriptional repressor in the regulation of *13-1* in liquid medium, as previously reported for regulation of the negative pathway controlling expression of the *lac-1* gene product (32, 34).

However, when examined by using a time course analysis, the kinetics and relative magnitude of cycloheximide-induced expression of *lac-1* and *13-1* in virus-free 13-1p(S)-GFP/EP155 differed (Fig. 8A and 8B). While *lac-1* accumulated to maximal levels of just greater than 10-fold that of the untreated culture at 24 h after addition of 3 μM cycloheximide, induction of *13-1* was more rapid and intense, peaking at a greater than 100-fold increase in accumulation at 6 h after addition of 3 μM cycloheximide before trailing off to nearly noninduced levels at 24 h (Fig. 8A and 8B). This suggests that not only are the inductive pathways regulating *13-1* and *lac-1* transcription different (i.e., CHV1-EP713 infection and cAMP-mediated transcriptional regulation for *13-1* and calcium/calmodulin/inositol trisphosphate-dependent signaling for *lac-1*), but the derepression of *13-1* and *lac-1* in liquid medium is also mediated through independent mechanisms.

Consistent with the observed hypovirus-mediated suppression of *lac-1* induction in 1.5% malt extract medium (Fig. 6A and 6B), cycloheximide-mediated transcriptional activation of *lac-1* was also inhibited in 13-1p(S)-GFP/EP155 infected with either CHV1-EP713 or CHV1-Euro7 (Fig. 9, upper panel, lanes 4 to 9). In contrast, *13-1* transcripts accumulated to even higher levels in the same virus-infected cultures in response to cycloheximide (Fig. 9, middle panel, lanes 4 to 9), further supporting differential regulation of the *lac-1* and *13-1* pathways. The amount of *13-1* message detected in the virus-infected cultures was independent of the virus strain, suggesting that culture conditions play a significant role in the observed differential effect of hypovirus strains on host gene expression.

## DISCUSSION

Two principal signal transduction pathways have been implicated in the manifestation of hypovirus-induced phenotypic changes for the pathogenic filamentous fungus *C. parasitica*: G-protein-linked, cyclic AMP-mediated (12, 15, 24) and calcium/calmodulin/inositol trisphosphate-dependent-signaling cascades (32, 34). Infectious chimeric cDNA clones of severe (CHV1-EP713) and mild (CHV1-Euro7) hypovirus strains have previously been used to map specific hypovirus symptom determinants responsible for altered fungal virulence, fungal growth, canker morphology, and asexual sporulation (13, 14). We have now taken a molecular and comparative virology approach to further define hypovirus-host interactions by linking distinct mild and severe hypovirus-induced phenotypes with the differential modulation of specific cellular signal transduction pathways.

With the transgenic *C. parasitica* promoter strain 13-1p(S)-

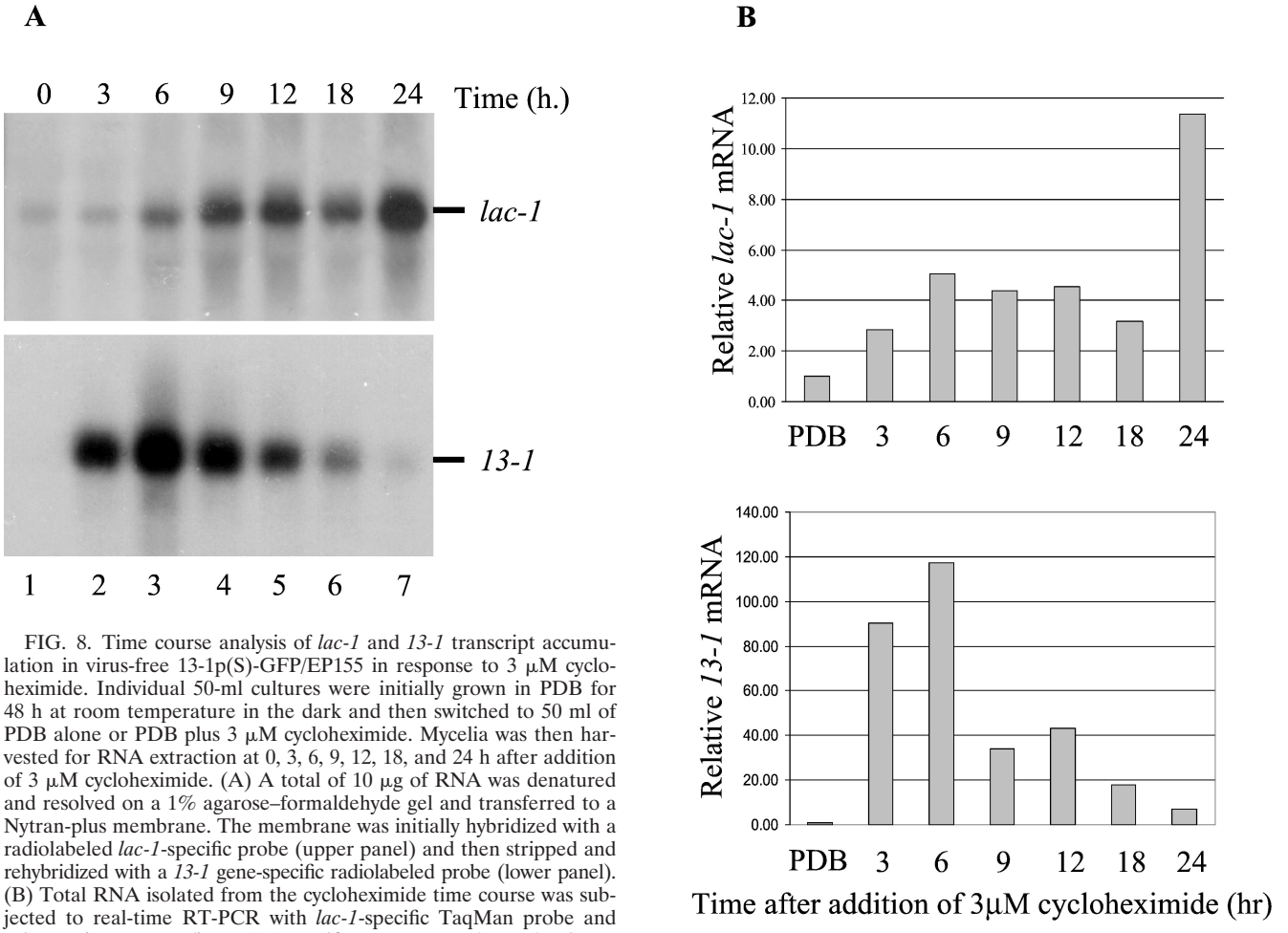


FIG. 8. Time course analysis of *lac-1* and *13-1* transcript accumulation in virus-free 13-1p(S)-GFP/EP155 in response to 3 μM cycloheximide. Individual 50-ml cultures were initially grown in PDB for 48 h at room temperature in the dark and then switched to 50 ml of PDB alone or PDB plus 3 μM cycloheximide. Mycelia was then harvested for RNA extraction at 0, 3, 6, 9, 12, 18, and 24 h after addition of 3 μM cycloheximide. (A) A total of 10 μg of RNA was denatured and resolved on a 1% agarose–formaldehyde gel and transferred to a Nytran-plus membrane. The membrane was initially hybridized with a radiolabeled *lac-1*-specific probe (upper panel) and then stripped and rehybridized with a *13-1* gene-specific radiolabeled probe (lower panel). (B) Total RNA isolated from the cycloheximide time course was subjected to real-time RT-PCR with *lac-1*-specific TaqMan probe and primers (upper panel) or *13-1*-specific TaqMan probe and primers (lower panel).

GFP/EP155, it was possible to demonstrate that cAMP-mediated, promoter-dependent cellular gene expression was activated by severe hypovirus CHV1-EP713 but not by the closely related mild hypovirus CHV1-Euro7. Additionally, it was possible to map the predominant viral determinant(s) mediating the activation of this pathway to a region encoded between nucleotides 5310 and 9897 of CHV1-EP713. Determinants for reduced radial growth on PDA-cellophane also mapped to this region of CHV1-EP713, linking a specific virus-induced trait with activation of a specific cellular signal transduction pathway.

Results of the chimera mapping studies also indicated that specific CHV1-EP713-induced traits could be uncoupled from virus-induced activation of cAMP-mediated gene expression. Chen et al. (13) have previously identified the region encoded between nucleotides 2363 and 5310 (i.e., the start of ORF B to the *Nar*I site) as containing a dominant determinant of canker morphology on chestnut tissue. In that study, *C. parasitica* infected with chimeras containing nucleotides 2363 to 5310 from CHV1-EP713 (R5 and R12) yielded cankers similar to those observed in the CHV1-EP713-infected strain. In contrast, *C. parasitica* infected with chimeras containing nucleotides 2363 to 5310 from CHV1-Euro7 (R6 and R10) yielded smaller versions of cankers initiated by the CHV1-Euro7-infected strain, displaying the characteristic raised canker margins and producing significantly more spore-containing pustules than the R5- and R12-infected fungi. The observation that R12 and R5 infection of 13-1p(S)-GFP/EP155 caused little or no *13-1* promoter-dependent GFP accumulation (Fig. 3C) suggests that CHV1-EP713-mediated suppression of asexual sporulation on infected chestnut tissue is independent of CHV1-EP713-mediated activation of cAMP-regulated gene expression.

Although the data presented do not provide direct evidence for the role of a specific virus-encoded enzymatic activity in the activation of cAMP-dependent signaling, it is possible to exclude both the p29 (nucleotides 496 to 1239) and p48 (nucleotides 2364 to 3617) proteinases and the putative RNA helicase (nucleotides 10336 to 11159). However, the region containing the activation determinant(s) does encode the viral RNA-dependent RNA polymerase. The 1,531-amino-acid polyprotein encoded within the region spanning nucleotides 5310 to 9897 of CHV1-EP713 and CHV1-Euro7 has an overall 94% amino acid identity (1,453 of 1,531 amino acids) and 96% similarity (1,494 of 1,531). Comparative sequence alignment reveals two regions of clustered dissimilarity. The first, a stretch of 281 amino acids encoded by nucleotides 6062 to

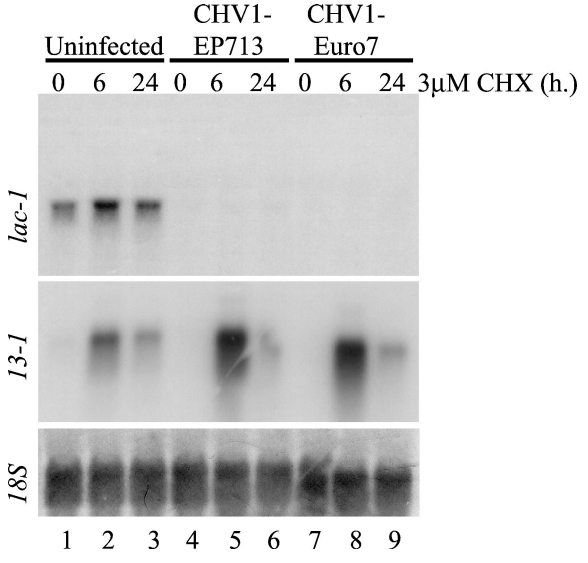


FIG. 9. Accumulation of *lac-1* and *13-1* transcripts in uninfected and CHV1-EP713- or CHV1-Euro7-infected 13-1p(S)-GFP/EP155 in response to 3 μM cycloheximide (CHX). Individual 50-ml cultures were initially grown in PDB for 48 h at room temperature in the dark and then switched to 50 ml of PDB alone or PDB plus 3 μM cycloheximide. Mycelium was then harvested for RNA extraction at 0, 6, and 24 h after addition of 3 μM cycloheximide, and 10 μg of RNA was denatured and resolved on a 1% agarose–formaldehyde gel and transferred to a Nytran-plus membrane. The membrane was initially hybridized with a radiolabeled *lac-1*-specific probe (upper panel) and then stripped and rehybridized with a *13-1* gene-specific radiolabeled probe (middle panel) or an 18S rRNA radiolabeled probe (lower panel).

6905, contains over half of the total dissimilar amino acids (18 of 37) within the 1,531 residues. This region is upstream of the predicted RNA-dependent RNA polymerase N-terminal boundary and encodes a protein of unknown function. The second cluster has a total of six unrelated amino acids in a stretch of 22. This sequence is located between conserved positive-strand viral RNA polymerase motifs IV and V of the CHV1-EP713 RNA-dependent RNA polymerase (31). The identification of these dissimilarity clusters provides opportunities for further detailed mapping of the activation determinant(s).

The mild and severe hypovirus strains were also found to differentially suppress extracellular laccase activity when infected cultures were grown on Bavendamm's medium (Fig. 5). By using chimeric hypoviruses R1 and R2, it was possible to localize the viral determinants regulating suppression of laccase activity on Bavendamm's medium to ORF B of CHV1-EP713. However, it was not possible to further dissect ORF B determinants regulating laccase activity, consistent with observations by Chen et al. (13) that CHV1-EP713 encodes multiple independent determinants for some virus-induced fungal phenotypic changes.

Surprisingly, the differential suppression of extracellular laccase activity by CHVEP713 and CHV1-Euro7 observed on Bavendamm plates did not extend to the calcium/calmodulin/inositol trisphosphate-dependent accumulation of *lac-1* transcript accumulation in malt extract, i.e., both strains were suppressive (Fig. 6). There are several plausible explanations for this difference. Since both LAC-1 (the *lac-1* gene product) and LAC-3 are thought to contribute to the laccase activity on tannic acid-containing medium (Bavendamm reaction), the observations presented in Fig. 5 and 6 would be predicted if CHV1-EP713 suppresses both LAC-1 and LAC-3 production while CHV1-Euro7 only suppresses the production of LAC-1. Additional possibilities are that laccase production is subject to control by different regulatory pathways under different culture conditions, that hypovirus-mediated suppression of laccase production is influenced by the culture conditions, or both.

There is considerable evidence to indicate that culture conditions, including light intensity, culture density, and growth medium composition, can have a significant effect on *C. parasitica* morphology and development, the magnitude and spectrum of virus-induced symptom expression, and fungal gene expression (16, 22, 27, 32, 33, 34). As noted in Fig. 1C, 8, and 9, the selection of growth medium had a dramatic effect on the differential accumulation of *13-1* promoter-dependent transcript accumulation in virus-free and severe and mild hypovirus-infected cultures. This may also be the case for the regulation of *lac-1* (Fig. 5 and 6). While a striking difference in many phenotypic characteristics can be observed between virus-free and hypovirus-infected *C. parasitica* when cultured either in planta or on solid medium such as PDA (13, 14, 27), CHV1-EP713 has been consistently reported to have little or no effect on fungal growth in liquid medium (30, 36, 55).

Significant differences in fungal growth, stress response, and other phenotypic traits have also been observed when *C. parasitica* strains disrupted in G-protein subunit genes are grown on PDA or in planta versus liquid medium (15, 24, 29; G. Segers and D. Nuss, unpublished observations). Thus, it is essential that the influence of culture conditions be carefully considered when investigating mechanisms underlying hypovirus-mediated modulation of host cell gene expression or regulatory pathways. The development of promoter-reporter constructs for monitoring specific regulatory pathways, as reported here, provides new opportunities for monitoring the effect of environmental conditions or hypovirus infection on specific cellular regulatory pathways. Coupled with future studies employing the use of microarray technologies, promoter-reporter fungal strains will facilitate the elucidation of a global view of alterations in the cellular regulatory circuitry, with the ultimate goal of monitoring hypovirus-mediated alterations of fungal gene expression in planta.

The observation that mild and severe hypovirus strains modulate different cellular signaling pathways has implications for engineering of hypoviruses for enhanced biological control potential. Hypoviruses that severely debilitate *C. parasitica* are not effective biological control agents because the resulting hypovirulent strains, while severely reduced in virulence, fail to persist and disseminate in the field (3). Chen et al. (13) have demonstrated the feasibility of selectively altering *C. parasitica* phenotypic traits, including the ability to colonize and produce spores on chestnut tissue, by infection with chimeric constructs of mild and severe hypovirus strains. A better understanding of the nature of viral symptom determinants and their relative effects on specific cellular regulatory pathways and expression of gene clusters will allow a more rational approach for engineering hypoviruses that exhibit a desired balance between virulence attenuation and ecological fitness.

## ACKNOWLEDGMENTS

We are grateful to Angus Dawe for critical review of the manuscript.

This work was supported in part by Public Health Service grant GM55981 to D.L.N. T.B.P. was a postdoctoral trainee on Public Health Service grant AI07510-3.

## REFERENCES

1. **Anagnostakis, S. L.** 1982. Biological control of chestnut blight. Science **215:**466–471.
2. **Anagnostakis, S. L.** 1984. Nuclear gene mutations in *Endothia* (*Cryphonectria*) *parasitica* that affect morphology and virulence. Phytopathology **74:**561–565.
3. **Anagnostakis, S. L., B. Chen, L. M. Geletka, and D. L. Nuss.** 1998. Hypovirus transmission to ascospore progeny by field-released transgenic hypovirulent strains of *Cryphonectria parasitica*. Phytopathology **88:**598–604.
4. **Anagnostakis, S. L., and P. R. Day.** 1979. Hypovirulence conversion in *Endothia parasitica*. Phytopathology **69:**1226–1229.
5. **Bavendamm, W.** 1928. Ueber das Vorkommen und den Nachweis von Oxydasen bei holzzerstörenden Pilzen. Z. Pflanzenschutz **38:**257–276.
6. **Bradford, M. M.** 1976. A rapid and sensitive method for quantification of microgram quantities of protein utilizing the principle of protein-dye binding. Anal. Biochem. **72:**248–254.
7. **Carpenter, C. E., R. J. Mueller, P. Kazmierczak, L. Zhang, D. K. Villalon, and N. K. Van Alfen.** 1992. Effect of a virus on accumulation of a tissue-specific cell-surface protein of the fungus *Cryphonectria* (*Endothia*) parasitica. Mol. Plant-Microbe Interact. **5:**55–61.
8. **Cenis, J. L.** 1992. Rapid extraction of fungal DNA for PCR amplification. Nucleic Acids Res. **20:**2380.
9. **Chen, B., C.-H. Chen, B. H. Bowman, and D. L. Nuss.** 1996. Phenotypic changes associated with wild-type and mutant hypovirus RNA transfection of plant pathogenic fungi phylogenically related to *Cryphonectria parasitica*. Phytopathology **86:**301–310.
10. **Chen, B., G. H. Choi, and D. L. Nuss.** 1993. Mitotic stability and nuclear inheritance of integrated viral cDNA in engineered hypovirulent strains of the chestnut blight fungus. EMBO J. **12:**2991–2998.
11. **Chen, B., G. H. Choi, and D. L. Nuss.** 1994. Attenuation of fungal virulence by synthetic infectious hypovirus transcripts. Science **264:**1762–1764.
12. **Chen, B., S. Gao, G. H. Choi, and D. L. Nuss.** 1996. Extensive alteration of fungal gene transcript accumulation and elevation of G-protein-regulated cAMP levels by a virulence-attenuating hypovirus. Proc. Natl. Acad. Sci. USA **93:**7996–8000.
13. **Chen, B., L. M. Geletka, and D. L. Nuss.** 2000. Using chimeric hypoviruses to fine-tune the interaction between a pathogenic fungus and its plant host. J. Virol. **74:**7562–7567.
14. **Chen, B., and D. L. Nuss.** 1999. Infectious cDNA clone of hypovirus CHV1-Euro7: a comparative virology approach to investigate virus-mediated hypovirulence of the chestnut blight fungus *Cryphonectria parasitica*. J. Virol. **73:**985–992.
15. **Choi, G. H., B. Chen, and D. L. Nuss.** 1995. Virus-mediated or transgenic suppression of a G-protein alpha subunit and attenuation of fungal virulence. Proc. Natl. Acad. Sci. USA **92:**305–309.
16. **Choi, G. H., T. G. Larson, and D. L. Nuss.** 1992. Molecular analysis of the laccase gene from the chestnut blight fungus and selective suppression of its expression in an isogenic hypovirulent strain. Mol. Plant-Microbe Interact. **5:**119–128.
17. **Choi, G. H., D. M. Pawlyk, and D. L. Nuss.** 1991. The autocatalytic protease p29 encoded by a hypovirulence-associated virus of the chestnut blight fungus resembles the potyvirus-encoded protease HC-Pro. Virology **183:**747–752.
18. **Churchill, A. C. L., L. M. Ciufetti, D. R. Hansen, H. D. Van Etten, and N. K. Van Alfen.** 1990. Transformation of the fungal pathogen *Cryphonectria parasitica* with a variety of heterologous plasmids. Curr. Genet. **17:**25–31.
19. **Craven, M. G., D. M. Pawlyk, G. H. Choi, and D. L. Nuss.** 1993. Papain-like protease p29 as a symptom determinant encoded by a hypovirulence-associated virus of the chestnut blight fungus. J. Virol. **67:**6513–6521.
20. **Dawe, A. L., and D. L. Nuss.** 2001. Hypoviruses and chestnut blight: exploiting viruses to understand and modulate fungal pathogenesis. Annu. Rev. Genet. **35:**1–29.
21. **Elliston, J. E.** 1978. Pathogenicity and sporulation in normal and diseased strains of *Endothia parasitica* in American chestnut, p. 95–100. *In* W. L. MacDonald, F. C. Cech, J. Luchok, and C. Smith (ed.), Proceedings of the American Chestnut Symposium. West Virginia University Press, Morgantown, W.Va.
22. **Elliston, J. E.** 1985. Characteristics of dsRNA-free and dsRNA-containing strains of *Endothia parasitica* in relation to hypovirulence. Phytopathology **75:**151–158.
23. **Gao, S., G. H. Choi, L. Shain, and D. L. Nuss.** 1996. Cloning and targeted disruption of *enpg-1*, encoding the major in vitro extracellular endopolygalacturonase of the chestnut blight fungus *Cryphonectria parasitica*. Appl. Environ. Microbiol. **62:**1984–1990.
24. **Gao, S., and D. L. Nuss.** 1996. Distinct roles for two G protein alpha subunits in fungal virulence, morphology, and reproduction revealed by targeted gene disruption. Proc. Natl. Acad. Sci. USA **93:**14122–14127.
25. **Gao, S., and D. L. Nuss.** 1998. Mutagenesis of putative acylation sites alters function, localization, and accumulation of a Gi alpha subunit of the chestnut blight fungus *Cryphonectria parasitica*. Mol. Plant-Microbe Interact. **11:**1130–1135.
26. **Gao, S., and L. Shain.** 1995. Activity of polygalacturonase produced by *Cryphonectria parasitica* in chestnut bark and its inhibition by extracts from American and Chinese chestnut. Physiol. Mol. Plant Pathol. **46:**199–213.
27. **Hillman, B. I., R. Shapira, and D. L. Nuss.** 1990. Hypovirulence-associated suppression of host functions in *Cryphonectria parasitica* can be partially relieved by high light intensity. Phytopathology **80:**950–956.
28. **Johnson, M. R., W. Kangsheng, J. B. Smith, M. J. Heslin, and R. B. Diaslo.** 2000. Quantitation of dihydropyrimidine dehydrogenase expression by real-time reverse transcription polymerase chain reaction. Anal. Biochem. **278:**175–184.
29. **Kasahara, S., and D. L. Nuss.** 1997. Targeted disruption of a fungal G-protein beta subunit gene results in increased vegetative growth but reduced virulence. Mol. Plant-Microbe Interact. **10:**984–993.
30. **Kazmierczak, P., P. Pfeiffer, L. Zhang, and N. K. Van Alfen.** 1996. Transcriptional repression of specific host genes by the mycovirus *Cryphonectria* hypovirus 1. J. Virol. **70:**1137–1142.
31. **Koonin, E. V., G. H. Choi, D. L. Nuss, R. Shapira, and J. C. Carrington.** 1991. Evidence for common ancestry of a chestnut blight hypovirulence-associated double-stranded RNA and a group of positive-strand RNA plant viruses. Proc. Natl. Acad. Sci. USA **88:**10647–10651.
32. **Larson, T. G., G. H. Choi, and D. L. Nuss.** 1992. Regulatory pathways governing modulation of fungal gene expression by a virulence-attenuating mycovirus. EMBO J. **11:**4539–4548.
33. **Larson, T. G., and D. L. Nuss.** 1993. Cyclophilin-dependent stimulation of transcription by cyclosporin A. Proc. Natl. Acad. Sci. USA **90:**148–152.
34. **Larson, T. G., and D. L. Nuss.** 1994. Altered transcriptional response to nutrient availability in hypovirus-infected chestnut blight fungus. EMBO J. **13:**5616–5623.
35. **MacDonald, W. L., and D. W. Fulbright.** 1991. Biological control of chestnut blight: use and limitation of transmissible hypovirulence. Plant Dis. **75:**656–661.
36. **McCabe, P. M., P. Pfeiffer, and N. K. Van Alfen.** 1999. The influence of dsRNA viruses on the biology of plant pathogenic fungi. Trends Microbiol. **1:**377–381.
37. **McCabe, P. M., and N. K. Van Alfen.** 1999. Secretion of cryparin, a fungal hydrophobin. Appl. Environ. Microbiol. **65:**5431–5435.
38. **Nuss, D. L.** 1992. Biological control of chestnut blight: an example of virus-mediated attenuation of fungal pathogenesis. Microbiol. Rev. **56:**561–576.
39. **Nuss, D. L.** 1996. Using hypoviruses to probe and perturb signal transduction processes underlying fungal pathogenesis. Plant Cell **8:**1845–1853.
40. **Nuss, D. L.** 2000. Hypovirulence and chestnut blight: from the field to the laboratory and back, p. 149–170. *In* J. W. Kronstad (ed.), Fungal pathology. Kluwer Academic Press, Dordrecht, The Netherlands.
41. **Prasher, D. C., V. K. Eckenrode, W. W. Ward, F. G. Prendergast, and M. J. Cormier.** 1992. Primary structure of the *Aequorea victoria* green fluorescent protein. Gene **111:**229–233.
42. **Puhalla, J. W., and S. L. Anagnostakis.** 1971. Genetics and nutritional requirements of *Endothia parasitica*. Phytopathology **61:**169–173.
43. **Rigling, D.** 1995. Isolation and characterization of *Cryphonectria parasitica* mutants that mimic a specific effect of hypovirulence-associated dsRNA on laccase activity. Can. J. Bot. **73:**1655–1661.
44. **Rigling, D., U. Heiniger, and H. R. Hohl.** 1989. Reduction of laccase activity in dsRNA-containing hypovirulent strains of *Cryphonectria* (*Endothia*) *parasitica*. Phytopathology. **79:**219–223.
45. **Rigling, D., and N. K. Van Alfen.** 1991. Regulation of laccase biosynthesis in the plant-pathogenic fungus *Cryphonectria parasitica* by double-stranded RNA. J. Bacteriol. **173:**8000–8003.
46. **Rigling, D., and N. K. Van Alfen.** 1993. Extra- and intracellular laccases of the chestnut blight fungus *Cryphonectria parasitica*. Appl. Environ. Microbiol. **59:**3634–3639.
47. **Sambrook, J., E. F. Fritsch, and T. Maniatis.** 1989. Molecular cloning: a laboratory manual, 2nd ed. Cold Spring Harbor Press, Cold Spring Harbor, N.Y.
48. **Shapira, R., G. H. Choi, and D. L. Nuss.** 1991. Virus-like genetic organization and expression strategy for a double-stranded RNA genetic element associated with biological control of chestnut blight. EMBO J. **10:**731–739.
49. **Shapira, R., and D. L. Nuss.** 1991. Gene expression by a hypovirulence-associated virus of the chestnut blight fungus involves two papain-like protease activities. Essential residues and cleavage site requirements for p48 autoproteolysis. J. Biol. Chem. **266:**19419–19425.
50. **Suzuki, N., L. M. Geletka, and D. L. Nuss.** 2000. Essential and dispensable virus-encoded replication elements revealed by efforts to develop hypoviruses as gene expression vectors. J. Virol. **74:**7568–7577.
51. **Van Alfen, N. K.** 1986. Hypovirulence of *Endothia (Cryphonectria) parasitica* and *Rhizoctonia solani*, p. 143–162. *In* K. W. Buck (ed.), Fungal virology. CRC Press, Boca Raton, Fla.

52. **Varley, D. A., G. K. Podila, and S. T. Hiremath.** 1992. Cutinase in *Cryphonectria parasitica*, the chestnut blight fungus: suppression of cutinase gene expression in isogenic hypovirulent strains containing double-stranded RNAs. Mol. Cell. Biol. **12:**4539–4544.
53. **Wang, P., and D. L. Nuss.** 1995. Induction of a *Cryphonectria parasitica* cellobiohydrolase I gene is suppressed by hypovirus infection and regulated by a GTP-binding-protein-linked signaling pathway involved in fungal pathogenesis. Proc. Natl. Acad. Sci. USA **92:**11529–11533.
54. **Zhang, L., R. A. Baasiri, and N. K. Van Alfen.** 1998. Viral repression of fungal pheromone precursor gene expression. Mol. Cell. Biol. **18:**953–959.
55. **Zhang, L., A. C. Churchill, P. Kazmierczak, D. H. Kim, and N. K. Van Alfen.** 1993. Hypovirulence-associated traits induced by a mycovirus of *Cryphonectria parasitica* are mimicked by targeted inactivation of a host gene. Mol. Cell. Biol. **13:**7782–7792.
56. **Zhang, L., D. Villalon, Y. Sun, P. Kazmierczak, and N. K. Van Alfen.** 1994. Virus-associated downregulation of the gene encoding cryparin, an abundant cell surface protein from the chestnut blight fungus *Cryphonectria parasitica*. Gene **139:**59–64.